

Lawrence Berkeley National Laboratory

Recent Work

Title

MESON MASS MEASUREMENTS I - THEORY OP THE MASS RATIO METHOD

Permalink

<https://escholarship.org/uc/item/2f88g7vf>

Author

Barkas, Walter H.

Publication Date

1953-09-01

eyd

UNIVERSITY OF
CALIFORNIA

*Radiation
Laboratory*

TWO-WEEK LOAN COPY

*This is a Library Circulating Copy
which may be borrowed for two weeks.
For a personal retention copy, call
Tech. Info. Division, Ext. 5545*

BERKELEY, CALIFORNIA

UCRL-2327
C.2

DISCLAIMER

This document was prepared as an account of work sponsored by the United States Government. While this document is believed to contain correct information, neither the United States Government nor any agency thereof, nor the Regents of the University of California, nor any of their employees, makes any warranty, express or implied, or assumes any legal responsibility for the accuracy, completeness, or usefulness of any information, apparatus, product, or process disclosed, or represents that its use would not infringe privately owned rights. Reference herein to any specific commercial product, process, or service by its trade name, trademark, manufacturer, or otherwise, does not necessarily constitute or imply its endorsement, recommendation, or favoring by the United States Government or any agency thereof, or the Regents of the University of California. The views and opinions of authors expressed herein do not necessarily state or reflect those of the United States Government or any agency thereof or the Regents of the University of California.

UCRL-2327

Unclassified - Physics Distribution

UNIVERSITY OF CALIFORNIA

Radiation Laboratory

Contract No. W-7405-eng-48

MESON MASS MEASUREMENTS I

THEORY OF THE MASS RATIO METHOD

Walter H. Barkas

September 16, 1953

Berkeley, California

MESON MASS MEASUREMENTS I
THEORY OF THE MASS RATIO METHOD
TABLE OF CONTENTS

	<u>Page</u>
Abstract.	3
I. Introduction.	4
II. Outline of Method.	7
III. The Particle Momentum	8
A. Orbit Calculations	8
B. Finite Target and Detector Effects	14
IV. The Particle Range	18
A. Energy Loss Processes	18
1. Energy Loss by Radiation	18
2. Energy Loss to Nuclei	18
3. Energy Loss to Electrons	20
B. Determination of the Momentum Exponent.	21
C. Range Straggling	24
1. Bohr Straggling and The Lewis Effect.	24
2. Heterogeneity Straggling	25 26
3. Distortion Straggling	25 26
4. Effects of Finite Grain Spacing and Grain Size	26 27
5. Effect of Shrinkage Factor	27 28
D. The Range Distribution Function.	29
V. Statistical Calculation of Mass Ratios	30
VI. Calculation of Muon Decay Momentum, Absolute Meson Masses, and the Electric Charge of Mesons	33
VII. Residual Effects	36
Acknowledgments	37
References.	38

MESON MASS MEASUREMENTS I
THEORY OF THE MASS RATIO METHOD

Walter H. Barkas
 Department of Physics, Radiation Laboratory
 University of California, Berkeley, California

September 16, 1953

ABSTRACT

The theory of particle mass-ratio measurement is ~~developed~~^{treated}. It applies particularly to the method developed at the University of California Radiation Laboratory in which measurements are made of particle ranges and momenta. A certain statistical variable, Rp^{-q} , is introduced. It is the quotient of the particle range and the q th power of its momentum, where q is that power (≈ 3.44) of the momentum which makes the expectation value of the quotient independent of the particle velocity in the velocity interval selected for the measurements. The expectation value of Rp^{-q} depends on the particle mass. The ratio of such expectation values for different particles at equal velocities provides a measure of the ratio of particle masses which does not depend on the exponent q , on the stopping material, or on the absolute value of the magnetic field employed to measure the momentum.

The theory of particle orbits in the non-uniform cyclotron field is worked out to provide the formulas from which momenta may be calculated, and to obtain the momentum distribution functions appropriate to the finite target and detector dimensions.

The energy loss processes in the nuclear track emulsion, which is used as a detector and stopping material, are studied, and the range-momentum exponent, q , found. A number of range straggling effects are evaluated. The theoretical distribution function of Rp^{-q} is studied, and the first three moments of the distribution calculated explicitly. The distribution is found to be essentially Gaussian. From the theory of the distribution of Rp^{-q} , the best estimate and the statistical uncertainty of the mass ratio (e. g., of meson to proton) are evaluated.

The measurement of the absolute decay momentum of the muon is also considered, and formulas for the best estimates of the absolute pion and muon masses derived. These contain only the pion to muon mass ratio and the absolute decay momentum.

MESON MASS MEASUREMENTS I

THEORY OF THE MASS RATIO METHOD

Walter H. Barkas

Department of Physics, Radiation Laboratory
University of California, Berkeley, California

September 16, 1953

I. INTRODUCTION

Meson mass determination presents special problems which have slowed the convergence of the numerous measurements.¹ One of the various reasons that precision is difficult to attain is that no known comparison particle with approximately the same specific charge as a meson is available, so that the utilization of doublets, analogous to those of atomic mass spectrometry, is not possible. Therefore, absolute measurements of quantities from which masses are calculated have usually been employed.

It was noticed, however, that a number of measurable quantities are normalized by the mass, so that when divided by the mass, they become functions of the velocity alone. For particles of the same charge, the energy (total or kinetic), the momentum, the range, the total ionization, the reciprocal of the mean scattering angle, and the range variance are such quantities. For nuclear track emulsion, two further quantities of this sort are the total number of developed grains in the track and its "integrated emptiness."² The way in which the mass appears in these measurable quantities suggests a means for determining the ratio of the meson mass to that of a comparison particle from relative measurements. For example, if the ratio of meson momentum to proton momentum is adjusted to be equal to the ratio of the mean meson range to the mean proton range, then the velocities are equal, and the mass ratio is equal to the common range and momentum ratio. The same argument applies for any pair of quantities each of which can be expressed as a product of the mass and a function of the velocity.

D. H. Perkins³ first suggested such a principle for determining the π to μ meson mass ratio from the observed numbers of developed grains in emulsion tracks as functions of the residual range. The derived mass in this

example is unfortunately very sensitive to counting errors, which may be both statistical and systematic, so that the grain count and range are not the most satisfactory pair of observable quantities for application of this principle. Using existing techniques, momentum and the rectified range in emulsion are probably the most useful quantities to employ for this purpose in spite of the inherent limitation set by range straggling. The method used in this experiment, which compares ranges and momenta of particles whose mass ratio is desired, was developed⁴ while seeking to eliminate so far as possible unknown or uncontrollable errors. An important feature of the analysis is the selection for statistical treatment of a function of the measured quantities whose distribution is substantially normal, and of which the moments are calculable.

Prior to the present measurement program, a considerable development of range and momentum methods⁵ for determining particle masses had been made, particularly by R. B. Brode and his collaborators. Because it was necessary to use cosmic rays, however, they did not enjoy a number of advantages which are gained when one can work with controlled particle sources in the strong and extensive magnetic field of the cyclotron vacuum chamber. Range plus ionization⁶ measurements, and range plus scattering⁷ measurements, as well as a few observations of momentum and momentum loss, momentum and electron collision, etc., have also been used to estimate meson masses.

Parallel to the employment of direct means for measuring meson masses, precise indirect methods have been developed which usually invoke the conservation laws for processes in which the meson is created or destroyed. Such methods ultimately may provide measurements of the highest precision, but it is important to insure at the outset that the reactions themselves are fully understood. Agreement of indirect results with those obtained directly may be put forward as strong evidence for the correctness of the hypothetical reaction (and equally for the validity of the assumptions employed in the direct method). Examples of such indirect meson mass measurements are the following: (a) mass of the μ^+ meson from the end point of its positron spectrum⁸; (b) mass of the π^+ meson by analysis of its production in proton-proton collisions⁹; (c) mass of the π^- meson from the energy of gamma rays associated with its capture in hydrogen¹⁰; and (d) mass of negative muon from energies of mesonic atom x-ray transitions.¹¹

The purpose of these articles, however, is to give an integrated account only of the "direct" mass ratio measurements made at the University of California Radiation Laboratory. The work will be presented in three parts. The first, this paper, discusses the principle of the method, the calculations, and the sources of error that may remain in it -- all with special reference to the experimental facilities and techniques that have been employed in this program. The measurements of pion masses and range straggling will be described by F. M. Smith in a second part, and the measurements of the positive muon mass and the energy balance in pion decay will be discussed by W. Birnbaum in a third paper. These papers constitute a complete report on this meson mass measurement program.

II. OUTLINE OF METHOD

The principle of the method is sketched in this section; the detailed treatment of each phase of the analysis will be taken up as separate topics.

The theory¹² of energy loss of a charged particle penetrating matter leads to an expression of the form:

$$dT/dR = f(\beta) \quad (1)$$

This form is valid in good approximation for the mean rate of energy loss of all particles that carry the same charge and that are massive compared to the electron. In Eq. 1, $f(\beta)$ is a function of the particle velocity, R is the residual range, and T is the kinetic energy. Since T is equal to the mass, μ , times a function of the velocity, Eq. 1 can be integrated. One obtains:

$$R/\mu = G(\beta) \quad (2)$$

A number of small corrections to Eqs. 1 and 2 are disregarded for the moment. They are treated in Section IV. Since the velocity is a function of p/μ , where p is the particle momentum, one can also write:

$$R/\mu = F(p/\mu) \quad (3)$$

In our experiments Ilford C2 emulsion was the material in which ranges were measured. Converting the range-energy relation for protons in emulsion to a range-momentum relation, one finds that the proton data can be expressed by:

$$R = c p^q \quad (4)$$

with c a constant for a given sample of emulsion, and q a slowly varying parameter which remains remarkably constant with a value of about 3.44 for protons of 25-40 Mev.

Combining equations (3) and (4) one obtains:

$$R/M = c (p/M)^q \quad (5)$$

where M is the mass expressed in units of the proton mass.

In determining a meson mass, one eliminates c by simultaneous measurements of the momenta and ranges of mesons and comparison particles such as protons. Priming quantities associated with the comparison particle and taking its mass to be unity, one obtains the following expression for the unknown mass:

$$M^{1-q} = (p/p')^{-q} R/R' \quad (6)$$

It is important to notice that when $R/R' = p/p'$, a special situation exists in which M is found correctly from Eq. 6 no matter what value of q is assumed. This experimental condition is attained when the velocity of the test particle is selected to be equal to that of the comparison particle.

In Eq. 6 only the ratios of ranges and momenta appear. It is an essential feature of the mass ratio method that the ranges of both types of particles be measured in the same body of stopping material and that momenta be measured in the same magnetic field. Then neither the emulsion stopping power nor the absolute intensity of the magnetic field enters into consideration in obtaining the mass ratio.

For the statistical treatment of the data we chose to study the experimental distribution of the quantity $R p^{-q}$ because, as will be seen, experimental conditions are attainable in which individual determinations of this function of the mass are distributed almost normally and with calculable moments about the mean value.

III. THE PARTICLE MOMENTUM

A. Orbit Calculations

In order to find particle masses by this method, one must measure momenta with good accuracy. The following calculations apply to all particles of charge e . The discussion, when it must be specific, relates to the situation in which the source of particles is a small target bombarded by the internal cyclotron beam, and the particles are detected in nuclear track emulsion. One can observe the point where the particle enters the surface of the emulsion. He can also measure the angles describing the direction of particle motion at the point of detection. With the empirically known magnetic field intensity function, these data are sufficient to determine the momentum, but because the field is not uniform, the precise calculation of the momentum requires a somewhat elaborate treatment.

It is simplest to describe the particle motion in cylindrical coordinates (r, ϕ, z) coaxial with the cyclotron field. The cyclotron field is assumed to have axial symmetry for the present calculations. The validity of this

assumption must be verified by appropriate measurements. First one considers orbits confined to the median plane where the magnetic field intensity is a function only of r . Then particles with small momentum describe trochoidal¹³ paths, as illustrated in Fig. 1, reaching a minimum radius R_1 and a maximum radius R_2 (the libration limits). Let (r_1, ϕ_1) be the point of origin (the target) and (r_2, ϕ_2) the point of detection. $(r \, d\phi/dr)_2$ is also obtained from the direction of the track at the point of detection. The dynamical problem¹⁴ is then treated by introducing the Lagrangian for the particle motion:

$$L = -\mu c^2 \left(1 - \frac{\dot{r}^2 + r^2 \dot{\phi}^2}{c^2} \right)^{1/2} + (e/c) \dot{\phi} \int_0^r r H(r) dr \quad (7)$$

Now $\dot{r}^2 + r^2 \dot{\phi}^2 = \beta^2 c^2$ is one constant of the motion.

Since ϕ is an ignorable coordinate, $\frac{d}{dt} \left(\frac{\partial L}{\partial \dot{\phi}} \right) = 0$, and

$$\frac{\mu r^2 \dot{\phi}}{(1 - \beta^2)^{1/2}} + e/c \int_{r_1}^r r H dr$$

is also a constant of the motion. Defining $\tan \lambda \equiv dr/r d\phi$, this constancy is expressed by:

$$r \cos \lambda = r_1 \cos \lambda_1 - 1/K \int_{r_1}^r r H dr, \quad (8)$$

where for the momentum $\mu \beta c (1 - \beta^2)^{-1/2} (= eH\rho/c)$ we have written $e/K/c$.

Since the point of detection lies on the orbit, we obtain

$$K = \frac{\int_{r_1}^{r_2} r H dr}{r_1 \cos \lambda_1 - r_2 \cos \lambda_2} \quad (9)$$

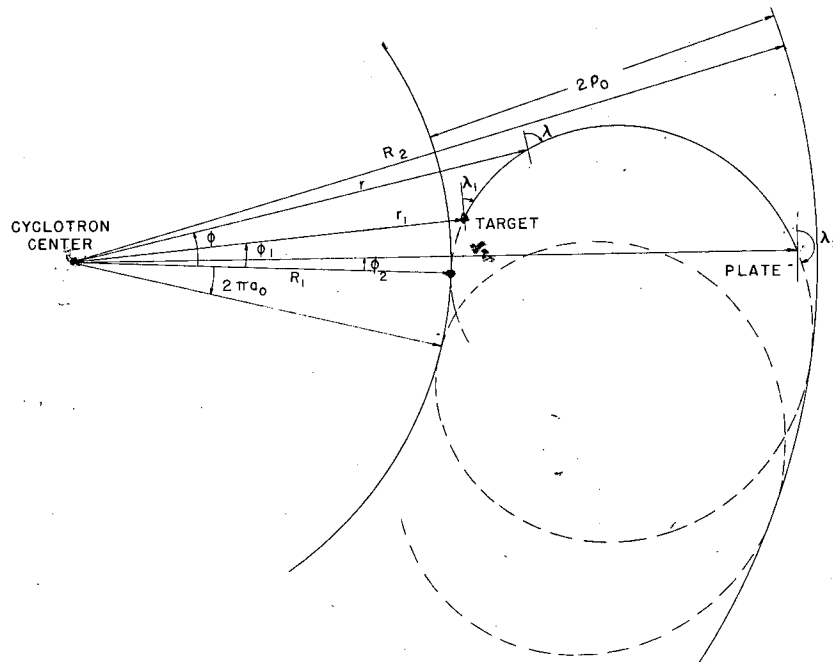


Fig. 1.

Diagram illustrating the trochoidal type of orbit in the median plane followed by a charged particle in the radially decreasing magnetic field of the cyclotron. The trochoidal path arises from the fact that the radius of curvature is larger where the magnetic field intensity is lower. The orbit is periodically tangent to the libration limits at radii R_1 and R_2 . All the quantities needed for an analysis of the orbit are labeled.

In this expression everything is observable except λ_1 .

The equation of the orbit is:

$$\phi = \int_{R_1}^r \frac{\cot \lambda \, dr}{r} \quad (10)$$

in which λ is the function of r given by Eq. 8.

The poles in the integrand may be avoided and the integration carried out¹⁴ by introducing a parameter, τ , given by:

$$\cos \tau = (R_2^2 + R_1^2 - 2r^2)/(R_2^2 - R_1^2)$$

The integrated form of the orbit is:

$$\phi = \arcsin \left(\frac{\rho_0 \sin \tau}{r} \right) + a_0 \tau + \sum_{n=1}^{\infty} a_n \sin n \tau \quad (11)$$

The a_1 and ρ_0 are defined below. If the magnetic field is described by an even polynomial in r (that odd powers do not enter may be inferred from the behavior of the cyclotron field at $r = 0$) as follows:

$$\frac{H(r) - H_0}{H_0} = h_0 + h_2 r^2 + h_4 r^4 \dots h_{2n} r^{2n} \equiv h(r),$$

then $\int_{R_1}^{R_2} r h dr = 0$, when $H_0 \equiv \frac{2}{R_2^2 - R_1^2} \int_{R_1}^{R_2} r H dr$.

Now $\rho_0 \equiv \frac{R_2 - R_1}{2}$, so $H_0 \rho_0 = K$. We also define $R \equiv \frac{R_1 + R_2}{2}$.

In terms of these quantities the a_1 may be calculated. Expressions for the first three follow:

$$a_0 = \rho_0^2 \left[h_2 + 2h_4 (R^2 + \rho_0^2) + 3h_6 (R^4 + 3R^2 \rho_0^2 + \rho_0^4) - 3\rho_0^2 h_2^2 - h_2 h_4 (7R^2 \rho_0^2 + 6\rho_0^4) + \dots \right]$$

$$a_1 = -R \rho_0^3 \left[\frac{4}{3} h_4 - \frac{3}{2} h_2^2 + 4h_6 (R^2 + \rho_0^2) - (6R^2 + 10\rho_0^2) h_2 h_4 + \dots \right]$$

$$a_2 = R^2 \rho_0^4 \left[\frac{h_6}{2} - h_2 h_4 + \dots \right]$$

The first term of Eq. 11 describes a circular orbit. The second superimposes a precession around the axis of symmetry, and the Fourier sum adds an harmonic perturbation of the precessing circular orbit. The orbit is periodically tangent to the libration circles of radii R_1 and R_2 .

Equation 11 for the orbit may be used to evaluate λ_1 under arbitrary conditions; for approximately 180° bending in a slowly varying field, with $\phi_1 = \phi_2 \approx 0$, the calculation is particularly simple. In this case

$$\lambda_1 \approx R\tau_1/r_1; \quad \pi - \lambda_2 \approx R(\pi - \tau_2)/r_2; \quad \text{so } \lambda_1 = (\pi - \lambda_2 + \lambda_0), \text{ where}$$

$$\lambda_0 \approx \pi/2 \frac{H_2 - H_1}{H_2 + H_1}, \text{ and}$$

$$K = \frac{\int_{r_1}^{r_2} r H dr}{r_1 \cos(\pi - \lambda_2 + \lambda_0) + r_2 \cos(\pi - \lambda_2)} \quad (12)$$

In Eq. 12 all quantities needed to determine K are measureable. A bending of 180° also enables one to measure momenta with the minimum error, as, in first approximation, the diameter of the orbit is observed directly, and the derived momentum is insensitive to the observed angle, λ_2 .

To simplify the momentum calculations one introduces a rectangular coordinate frame with the x-axis lying along a radial line extending toward larger radii and the z-axis parallel to the field axis. The origin is at the center of the target and measurements are made with apparatus designed so that the center of the detecting plate lies in the xz plane. The angle θ , defined below, and x_0 , the x coordinate at which the orbit crosses the x-axis, are then found with negligible error from the track position and direction.

For a particle starting at the center of the target:

$$K = \frac{\int_{r_1}^{r_1 + x_0} rHdr}{r_1 \cos(\theta' + \lambda_0) + (r_1 + x_0) \cos \theta'} \quad (13)$$

In this expression θ' is the angle to the y-axis measured in the xy plane at which the orbit crosses the x-axis; θ' is positive when the orbit has not yet reached the outer libration limit. In our experiments λ_0 is entirely negligible for the meson orbits but not for the proton orbits. For mesons, therefore:

$$K = \frac{\sec \theta' \int_{r_1}^{r_1 + x_0} rHdr}{2r_1 + x_0}$$

If the angle of the orbit to the median plane (the xy plane) is γ_0 , then $(e/c)K \sec \gamma_0$ is the total momentum of a particle which starts at the center of the target. The quantity

$$\frac{\sec \gamma_0 \int_{r_1}^{r_1 + x_0} rHdr}{2r_1 + x_0}$$

may be expressed graphically as a function of x_0 , so that the momentum calculations become much simplified.

Some attention must be given to the component of particle motion perpendicular to the median plane. In the present experiments this component of velocity is always small and the composition of it with the component parallel to the median plane is accomplished in multiplying eK/c by $\sec \gamma_0$, where γ_0 has been assumed constant along the orbit. To test the validity of this procedure, it will suffice to estimate the deviation from constancy of the velocity component perpendicular to the median plane.

If \dot{z}_1 is the initial component of velocity parallel to the z axis and Δz is the maximum change in this component, then it is readily shown that:

$$\Delta \dot{z} / \dot{z}_1 \approx (\pi/2 - 1) \rho_0 n/R \quad \text{where } n = -r/H \partial H_z / \partial r .$$

Here n has been assumed constant. Actually it varies slowly, but it has a maximum value in our experiments of 0.07, so even for proton orbits with $\rho_0 \approx R/3$, the maximum deviation from constancy of \dot{z} is not more than one percent. Therefore one can safely treat the two components of velocity as independent.

B. Finite Target and Detector Effects

The apparent momentum, p , is calculated assuming that the particle starts at the center of the target and that its orbit crosses the xz plane at a definite value ($-z_0$) of z . Actually in the experiments the target has usually been made in the form of a rectangular parallelepiped of dimensions $2a$, $2b$, and $2c$ in the x , y and z directions, respectively. Furthermore particles are accepted for measurement with θ lying in a finite interval, and they strike the surface of the emulsion anywhere in the searched area, which is symmetrically located with respect to the x axis. Particles with a distribution of true momenta p_1 contribute to the group with apparent momentum p . Consequently, one must study the function $U(p_1, p)$, which gives the probability, $U(p_1, p) dp_1$, that the true momentum lies between p_1 and $p_1 + dp_1$ when the apparent momentum is p . The question may be treated in a general manner by calculating:

$$\langle p_1^n \rangle = \int p_1^n U(p_1, p) dp_1 = p^n (1 + \omega_n) \quad (14)$$

In the design of the experiments ω_n is made as small as possible. It is evaluated as follows: With the origin at the center of the target, the orbit is assumed to begin at the point (x, y, z) and is observed to cross the x axis near the outer libration limit at $x = x_0$, making an angle θ with the y axis. The emulsion surface is assumed to lie in the plane $z = -z_0 - \epsilon y'$ with $x_0 \gg z_0$ and $\epsilon \ll 1$. The particle is observed to enter the emulsion at a point having a y coordinate equal to y' .

On carrying out the expansions through third order in the small quantities z_0/x_0 , x/x_0 , y/x_0 , z/x_0 , y'/x_0 , θ' and ϵ we find the following terms remaining in ω_n :

$$\begin{aligned}
 & - \frac{n\langle x \rangle}{x_0} \\
 & + \left(\frac{n(n-1)\langle x^2 \rangle}{2x_0^2} + \frac{n\langle y \times \theta' \rangle}{x_0} + \frac{n\langle y^2 \rangle}{x_0^2} + \frac{2n\langle z^2 \rangle}{\pi^2 x_0^2} + \frac{4nz_0\langle z \rangle}{\pi^2 x_0^2} \right) \\
 & + \left(\frac{8nz_0^2}{3x_0^2} \langle \theta' \rangle + \frac{8nz_0^2}{3x_0^3} \langle y \rangle + \frac{8nz_0^2}{3x_0^3} \langle y' \rangle + \frac{16nz_0}{3x_0^2} \langle z \times \theta' \rangle + \frac{16nz_0}{3x_0^3} \langle yz \rangle + \frac{16nz_0}{3x_0^3} \langle z \times y' \rangle \right) \\
 & + \frac{8n}{3x_0^2} \langle z^2 \times \theta' \rangle + \frac{8n}{3x_0^3} \langle yz^2 \rangle + \frac{8n}{3x_0^3} \langle z^2 \times y' \rangle + \frac{4nz_0^2}{\pi^2 x_0^3} \langle x \rangle - \frac{n(n-1)}{x_0^2} \langle xy \times \theta' \rangle \\
 & + \frac{4n\epsilon \langle y \times z \rangle}{\pi^2 x_0^2} + \frac{4n\epsilon z_0 \langle y \rangle}{\pi^2 x_0^2} - \frac{n(n-2)\langle xy^2 \rangle}{x_0^3} \\
 & - \frac{2n(n-2)}{\pi^2 x_0^3} \langle xz^2 \rangle - \frac{4n(n-2)z_0 \langle xz \rangle}{\pi^2 x_0^3} - \frac{n(n-1)(n-2)}{6} \frac{\langle x^3 \rangle}{x_0^3} \Big)
 \end{aligned}$$

For future reference we also calculate:

$$\begin{aligned}
 \omega_{2q} - 2\omega_q = q^2 \left[\frac{\langle x^2 \rangle}{x_0^2} - \frac{2\langle xy \rangle}{x_0^2} - \frac{2\langle xy^2 \rangle}{x_0^3} - \frac{4\langle xz^2 \rangle}{\pi^2 x_0^3} - (q-1) \frac{\langle x^3 \rangle}{x_0^3} \right. \\
 \left. - \frac{8z_0 \langle xz \rangle}{\pi^2 x_0^3} \right]
 \end{aligned}$$

and

$$\omega_{3q} - 3\omega_{2q} + 3\omega_q = -q^3 \frac{\langle x^3 \rangle}{x_0^3}$$

In these expressions the mean or expectation value of a statistical quantity, Q , is written $\langle Q \rangle$.

The distributions of θ' and y' are observed, The distributions of x , y , and z must be inferred from the geometry of the target and other information relating to the problem. In the case of μ^+ mesons, all the particles are assumed to arise from the decay of π^+ mesons which stop in a very thin layer on the surface of the target. No negative values of θ' can be associated with muons coming from the surface $x = +a$, and no positive values of θ' are associated with muons coming from the surface $x = -a$. One actually observes a number N^+ with θ' positive and N^- with θ' negative. For protons and pions it is assumed that the orbits start with equal probability anywhere in the target. This is a justified assumption because on the one hand measurements of the radioactivity throughout the target show the activity to be uniform, and on the other hand the nature of the low-energy pion spectrum is fairly well described by stating that the number of mesons per unit range interval is approximately constant. The energy loss in the target, then, has little effect on the distribution of positions from which the mesons come. In all cases the finite target effects are small, and for the protons they are almost completely negligible. In Table I the various calculated mean values have been listed. For protons the calculations were made for a cylindrical target of radius r_0 and length $2c$.

Table I

Mean Values of Statistical Quantities for $z_0 \gg c$

	Pions	Muons	Protons
$\langle x \rangle$	0	$\frac{N^+ - N^-}{N^+ + N^-} \frac{ab}{(a + b)}$	0
$\langle x^2 \rangle$	$a^2/3$	$\frac{a^2 (a + 3b)}{3 (a + b)}$	$r_0^2/4$
$\langle y \rangle$	0	$\frac{ab}{a + b}$	0
$\langle y^2 \rangle$	$b^2/3$	$\frac{b^2 (b + 3a)}{3 (a + b)}$	$r_0^2/4$
$\langle z \rangle$	$c^2/3z_0$	$c^2/3z_0$	$c^2/3z_0$
$\langle z^2 \rangle$	$c^2/3$	$c^2/3$	$c^2/3$
$\langle xy \rangle$	0	0	0
$\langle xz \rangle$	0	$\frac{abc^2(N^+ - N^-)}{3z_0 (a + b) (N^+ + N^-)}$	0
$\langle yz \rangle$	0	$\frac{abc^2}{3z_0 (a + b)}$	0
$\langle xz^2 \rangle$	0	$\frac{1}{3} \frac{N^+ - N^-}{N^+ + N^-} \frac{abc^2}{(a + b)}$	0
$\langle yz^2 \rangle$	0	$\frac{abc^2}{3(a + b)}$	0
$\langle x^3 \rangle$	0	$\frac{(N^+ - N^-)}{(N^+ + N^-)} \frac{a^3 b}{(a + b)}$	0
$\langle xy^2 \rangle$	0	$\frac{(N^+ - N^-)}{3(N^+ + N^-)} \frac{ab^3 (b + 3a)}{(a + b)^2}$	0

IV. THE PARTICLE RANGE

A. Energy Loss Processes

Three effects contribute to the average rate of energy loss of a charged-particle penetrating matter. For our experiments they are, in ascending importance: (a) radiation loss, (b) energy loss to nuclei, and (c) energy loss to electrons. We wish to examine these processes in sufficient detail that we may make appropriate corrections if necessary to the simple equations 1 and 2.

1. Energy Loss by Radiation

In traversing emulsion the space rate at which energy is radiated by a nonrelativistic particle of charge e is approximately:¹⁵

$$\frac{16}{3} \frac{e^2}{hc} \left(\frac{e^2}{mc^2} \right)^2 \frac{m}{\mu} \sum_t N_t Z_t^2 \quad \text{mc/cm}^2 \quad (16)$$

where μ is the particle mass, m the electron mass, and N_t is the number of nuclei of atomic number Z_t per cubic centimeter in the emulsion. From the known composition of the emulsion we obtain for the rate of energy loss:

$$\approx \frac{3.1 \times 10^{-5}}{M} \text{ Mev/cm ,}$$

where M is the particle mass expressed in units of the proton mass. For a proton of 33 Mev or for a meson of the same velocity, the energy lost by radiation in coming to rest is therefore only $\approx 1.5 \times 10^{-5}$ Mev. It is consequently quite negligible. At the lowest velocities the Born approximation method of calculation employed in deriving Eq. 16 fails, but more exact calculations¹⁵ do not change the order of magnitude of the energy loss.

2. Energy Loss to Nuclei

In the nonrelativistic region one may estimate that the energy, ΔT_n , absorbed by transfer of momentum to nuclei of the emulsion in an element of path ΔS from a particle carrying charge e at velocity βc is:

$$\Delta T_n = \frac{4\pi e^4}{\beta^2 c^2} \Delta S \sum_t \frac{N_t Z_t^2}{M_t} \ln b_t/a_t \quad \text{ergs} \quad (17)$$

In this expression, as before, N_i is the number of atoms per cubic centimeter of atomic number Z_i and mass M_i in the emulsion. Also, b_i and a_i are the usual ¹⁶ maximum and minimum impact parameters for the i th type of atom in the stopping material.

On the other hand, the mean square angle of nuclear coulomb scattering ¹⁶ (considered small) in a path ΔS experienced by a particle of mass μ , is given by:

$$\langle \phi^2 \rangle = \frac{8\pi e^4}{\mu^2 c^4 \beta^4} \Delta S \sum_i N_i Z_i^2 \ln b_i/a_i \quad (18)$$

The connection between energy loss to nuclei and nuclear scattering is an intimate one. Whereas the scattering can be observed, the energy loss to nuclei is difficult to measure directly. We shall use Eqs. 17 and 18 to relate them. For convenience an effective mass \bar{M} is defined as follows:

$$1/\bar{M} = \frac{\sum_i \frac{N_i Z_i^2}{M_i} \ln a_i/b_i}{\sum_i N_i Z_i^2 \ln a_i/b_i} \approx \frac{\sum_i N_i Z_i^2/M_i}{\sum_i N_i Z_i^2}$$

From the composition of Ilford c_2 emulsion, one calculates:

$$\bar{M} \approx 75 \mu_p, \text{ where } \mu_p \text{ is the proton mass.}$$

Then from Eqs. 17 and 18:

$$\frac{\Delta T_n}{T} = \frac{\mu}{\bar{M}} \langle \phi^2 \rangle \approx \frac{M}{75} \langle \phi^2 \rangle$$

This is really an upper limit for the energy loss to nuclei, since some collisions of large impact parameter may contribute slightly to the scattering, but are adiabatic and transfer no energy. There is in addition a small electron effect. The mean projected angle $\langle \alpha \rangle$ in degrees between successive chords is a well known empirical quantity.

It is given ¹⁷ by:

$$\langle \alpha \rangle \approx \frac{25}{p \beta c} \left(\frac{\Delta S}{100} \right)^{\frac{1}{2}}$$

with ΔS in microns and $p\beta c$ in Mev. Noting that $\langle \alpha^2 \rangle = \frac{\pi^3}{21,600} \langle a \rangle^2$, *(for a gaussian distrib.)*

then in the nonrelativistic approximation:

$$\Delta T_n = \frac{6.4 \times 10^{-8}}{\beta^2} \Delta S \quad \text{Mev.}$$

The rate of energy loss to nuclei depends only on the velocity if the few tracks that suffer large-angle scattering are excluded from measurement. The form of Eq. 1 is therefore preserved for this type of energy loss.

The actual magnitude of the energy loss to nuclei is also small. Taking $\beta^2 \approx \frac{T}{469 M}$ where M is in units of the proton mass, and $T/M = .251(R/M)^{.581}$, an empirical range-energy in emulsion,¹⁸ we obtain:

$$\Delta T_n \approx 1.2 \times 10^{-4} (R/M)^{-.581} \Delta S \quad \text{Mev.}$$

On integrating, the total energy loss to nuclei, T_n , is found:

$$T_n/M \approx 2.8 \times 10^{-4} (R/M)^{.419} \quad \text{Mev.} \quad (19)$$

For a particle with $\beta = 0.26$, T_n/M amounts to only 10^{-2} Mev.

Because the form of Eq. 1 is not altered, and the whole effect is small, no correction for energy loss to nuclei is required.

3. Energy Loss to Electrons

Interaction with electrons is the predominant energy loss process for fast charged particles penetrating emulsion. Other effects have been evaluated above for assurance that they are negligible.

For a composite stopping material such as emulsion, the usual¹² expression for the mean rate of energy loss of a fast particle to electrons becomes:

$$-\left\langle \frac{dT}{dX} \right\rangle = \frac{4\pi}{\beta^2} \left(\frac{e^2}{mc^2} \right)^2 \left(\sum_i N_i Z_i \right) \ln \frac{2mc^2 \beta^2 e^{-\beta^2}}{\bar{I} \left(1 + \frac{m}{\mu}\right)^2 (1 - \beta^2)} \quad m_0^2/c^2 \quad (20)$$

In this expression \bar{I} is defined by

$$\ln \bar{I} = \sum_i N_i Z_i \ln I_i / \sum_i N_i Z_i, \text{ where } I_i$$

is the appropriate mean ionization potential of the i th type of atom in the emulsion. I/Z is a slowly varying function of Z . Using the data of Bakker and Segre¹⁹, I was determined graphically for each element in the emulsion from the curve of I/Z vs. Z . Assuming the stated composition of Ilford C2 emulsion, \bar{I} was found to be 270 ev.

B. Determination of the Momentum Exponent

Equation 20 is not expected to hold at very low velocities, but we assume its form for protons above 5 Mev. The empirical range-energy data obtained from various sources are quite consistent for protons of 5 Mev. The range is given as 171.9 μ by Cüer²⁰, 172.5 μ by Wilkins²¹, and 171.4 μ by Rotblat²². We adopt 172 μ as the range of a 5-Mev proton. We also possess a considerable amount of information on the range of protons in the vicinity of 33.6 Mev. Each of the plates used in obtaining the pion/proton mass ratios in our experiment provides groups of protons whose ranges and absolute momenta are accurately known. From them we obtain a reliable range of $4580 \pm 18 \mu$ at 33.64 Mev. (This range is somewhat lower than that previously measured¹⁸. The older measurement was made with plates in equilibrium with the atmosphere at a relative humidity of 55 percent. This is believed to be too high to be representative of normal C2 emulsion. Below 50 percent relative humidity the range is rather insensitive²³ to the humidity. In these experiments the moisture content of the plates was slightly lower than that at which the plates are received. After being unwrapped, the plates were closely packed in another sealed box for the period before use. They were subjected to evacuation for about twenty minutes immediately prior to exposure, but we know from other experiments²³ that the diffusion of moisture out of the emulsion is small during this period of evacuation.)

Using $\bar{I} = 270$ ev., we integrate Eq. 20 between the limits of 5 Mev and 33.64 Mev to evaluate $\sum_i N_i Z_i$. We find $\sum_i N_i Z_i = 1.00 \times 10^{24}/\text{cc}$. From the

assumed composition of the emulsion, the number of electrons per cubic centimeter is 1.07×10^{24} . The difference probably arises chiefly from a well known effect: the more tightly bound electrons are not fully effective in stopping. In the interval 5-30 Mev, the K electrons of Br and Ag do not contribute to the energy loss. Some deviation from the stated composition of the emulsion is also possible; we know the water content to be variable.

One can now calculate the value of the exponent, $q \equiv \frac{p}{R} \frac{dR}{dp}$, as a function of the proton energy. This relationship is shown in Fig. 2. The stability of q is remarkable. It remains between 3.44 and 3.45 throughout the proton energy interval 23-42 Mev. The particle velocity chosen for our experiments corresponds to a proton energy of about 33.6 Mev. In this vicinity q passes through a maximum.*

Neutralization of the charge of a positive particle at low velocities will slightly increase its mean range relative to that of a negative particle, but here this effect is negligible.²⁵

It is possible that the stopping power of the emulsion is to a slight extent a function of depth in the emulsion. In these experiments the dip angle of the shorter tracks is greater than that of the long tracks in such a way that the effect, if it existed, would be largely eliminated.

*Since the above stopping effects were calculated, a paper by Vigneron²⁴ has appeared in which he concludes from a more elaborate study of the empirical information at lower velocities that the Bakker and Segrè potentials are too low. His calculated curve fits our high-energy point precisely, as well as being consistent with the best low-energy data. Vigneron's range-energy curve, therefore, probably is reliable. The value of q calculated from his data is 3.46. If one used this figure rather than the adopted value of 3.44, the effect on the derived masses would be negligible.

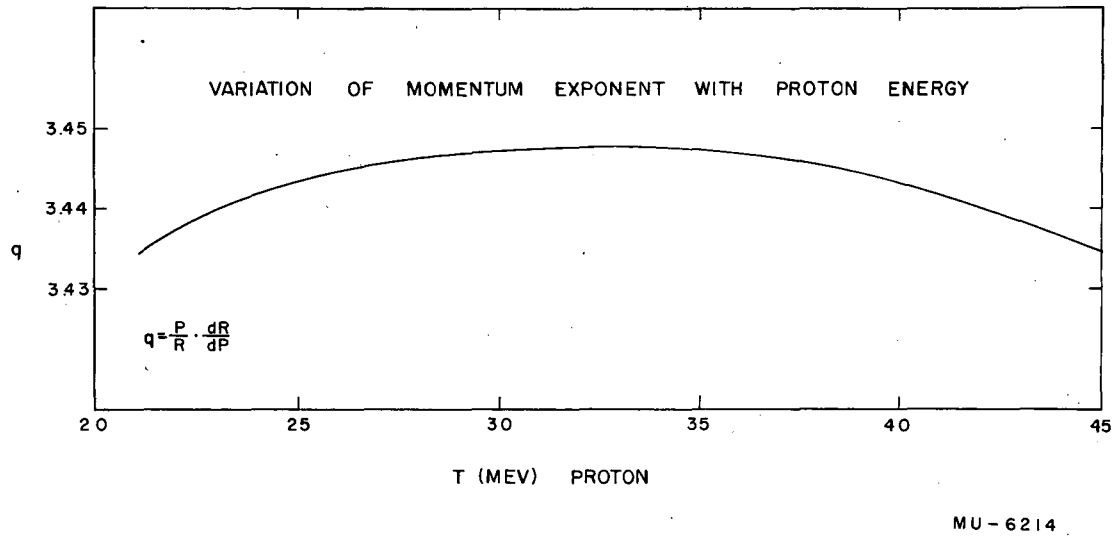


Fig. 2.
Variation of Momentum Exponent
with Proton Energy.

C. Range Straggling

1. Bohr Straggling and The Lewis Effect

It is well known that the individual ranges of similar particles, all of the same initial momentum, are not all the same, but are distributed about a mean range. The magnitude of the range straggling in homogeneous materials was calculated by Bohr²⁶ from the statistics of the energy-loss process. Refinements of the calculations have not greatly altered his estimate of the range straggling. This straggling, according to Bohr, contributes a range variance of:

$$\beta_2 = 4\pi \left(\sum_l N_l Z_l \right) e^4 \int_0^T \frac{dT}{(dT/dR)^3} \quad (21)$$

The individual energy losses in collisions with electrons are distributed in a highly unsymmetrical manner, but the distribution of ranges, in accord with the central limit theorem²⁷, tends toward normality when many separate collisions are required to stop the particle. H. W. Lewis²⁸ has recently re-examined the range straggling and evaluated the moments of the range distribution in a rather satisfactory manner. He obtains the same result as Bohr for the range variance. Equation 21 may be integrated by using for T the empirical expression²³ $T = .251 M^{.419} \langle R_1 \rangle^{.581}$. In this form T is in Mev, M in units of the proton mass, and $\langle R_1 \rangle$ is the measured mean range in microns. One then obtains (putting $\sum_l N_l Z_l = 1.03 \times 10^{24}/\text{cc}$; the K electrons of Ag and Br are assumed not to contribute to the straggling):

$$\beta_2/M = 6.8 \times 10^{-4} (\langle R_1 \rangle/M)^{1.838} \quad (22)$$

β_2 is expressed in (microns)².

A small skewness is also expected in the range distribution. A measure of the asymmetry of ranges is obtained if one computes $\beta_3 \equiv \langle (R_1 - \langle R_1 \rangle)^3 \rangle$. Using the method of Lewis, one may derive the relation:

$$\frac{d\beta_3}{d\langle R_1 \rangle} = \left(\frac{d\beta_2}{d\langle R_1 \rangle} \right)^2 \left(2.3 - .58 \ln \frac{\langle R_1 \rangle}{M} \right)$$

2. Heterogeneity Straggling

The emulsion consists of bodies of silver halide embedded in gelatin. Since the stopping powers of these two materials are not the same, the particle ranges tend to fluctuate. Clearly if more than the normal part of a path happens to be in gelatin, the range will be extended, and conversely. For the purpose of estimating the heterogeneity effect, one may assume that the silver halide is in the form of spheres of diameter d distributed with uniform average density throughout the emulsion. One may also assume that the number of spheres traversed by the moving particle in a fixed element of path is given by a binomial distribution. The variance of a binomial distribution is probably somewhat too high to be correct for concentrated emulsion where randomness is inhibited by contact between adjacent silver halide crystals, but a closer approximation is difficult to obtain. A detailed calculation employing the binomial distribution gives for the range variance, σ_H^2 , arising from the heterogeneity effect:

$$\sigma_H^2 = \frac{(r-1)^2 (S-1) (S+8)}{12 [1+r (S-1)]^2} d \langle R_1 \rangle,$$

where $\langle R_1 \rangle$ is the mean range, S is the ratio of emulsion volume to gelatin volume (approximately the shrinkage factor), r is the ratio of the ranges which would be found in gelatin and silver bromide separately, and d is the mean grain diameter. Winand²⁹ has measured d for C2 emulsion by electron microscopy. He finds $d \approx 0.2\mu$. If we assume $r \approx 4$ and $S \approx 2$, then:

$$\sigma_H^2 \approx 0.06 \langle R_1 \rangle^2 \text{ (microns)}^2.$$

For the present experiments this is a small effect.

3. Distortion Straggling

If the latent images of a number of tracks all have the same length in the emulsion before processing and are parallel to the emulsion surface, the tracks will not even then all have the same length after processing. First, the emulsion may have dried originally with strains in it which are relieved in the processing. Other strains may be introduced on drying again. Such effects may be directional. In addition, a violent small-scale distortion certainly takes place, because the fixer dissolves out the silver halide crystals which

occupy about half the volume of the emulsion. The spaces left are filled by the collapse of the gelatin with attendant microscopic distortions. The amount of this type of distortion is also affected by the water content of the emulsion.

The large-scale distortions do not lend themselves to theoretical analysis, and they must be avoided by good technique. The small-scale distortions are unavoidable, but if the dimensions of the local regions of distortion are small compared to the track length, then one may deduce that the cumulative effect of these local distortions along the track should produce a range variance proportional to the range (at least for moderate ranges so that the attachment of the gelatin to the glass does not limit the variance). Defining σ_d^2 as the distortion range variance, we have:

$$\sigma_d^2 = k \langle R_1 \rangle,$$

where k is a constant for the particular sample of emulsion. The small-scale distortion effect cannot be distinguished from the heterogeneity straggling. Seifert³⁰ has observed effects which can be interpreted as distortion straggling, and all range measurements in emulsion must suffer to some extent from this effect. The unusually large straggling of μ^+ meson ranges found by Fry and White³¹ probably is at least partially explainable if one assumes significant distortion effects.

4. Effects of Finite Grain Spacing and Grain Size

If the particle is not strongly ionizing on entering the emulsion, the grains rendered developable may be separated by distances which are not negligible. If the mean grain spacing is λ , then the probability of not producing a grain in a distance x is $\approx e^{-x/\lambda}$. The tracks will appear shortened systematically by an amount λ , and an additional range variance of λ^2 will be introduced. At the end of the track where the particle stops, the grains are usually dense, and this correction may be disregarded.

The finite grain size causes an additional uncertainty at the beginning and end of the track, but since the diameter of C.2 grains is $\approx 0.2\mu$, no corrections for this effect are justified in our experiments.

28
27

If the surface of the emulsion is rough a further error is introduced in determining the point of entry. To check this, optical tests have been made on the surface. When an optically flat piece of glass is laid on the surface, interference fringes are visible and widely spaced so that no correction for roughness effects seem necessary.

5. Effect of the Shrinkage Factor

On processing the emulsion, we find that its thickness is reduced because the silver halide is removed. The ratio of the thickness of the unprocessed emulsion to the processed thickness is the shrinkage factor S_o .

If the true shrinkage factor is S_o and it is incorrectly assumed to be S , then to an element of path of true length δ , a length

$\left(1 + \frac{S^2 - S_o^2}{S_o^2} \sin^2 \gamma_1\right)^{1/2} \delta$ will be attributed. In this expression γ_1

is the angle of dip, the angle between an element of the track and the plane of the emulsion surface before processing.

One then obtains for the range error ΔR arising from the shrinkage factor error:

$$\frac{\Delta R}{\langle R_1 \rangle} \approx \frac{S - S_o}{S_o} \langle \sin^2 \gamma_1 \rangle, \text{ where by } \langle \sin^2 \gamma_1 \rangle \text{ is meant the mean value}$$

of $\sin^2 \gamma_1$ along the path.

An incorrect choice of the shrinkage factor also introduces a source of variance into the range measurement. From this cause a range variance σ_γ^2 is contributed, where:

$$\sigma_\gamma^2 \approx \left(\frac{S - S_o}{S_o}\right)^2 \langle R_1 \rangle^2 \left(\langle \sin^4 \gamma_1 \rangle - \langle \sin^2 \gamma_1 \rangle^2\right)$$

This is usually negligible compared to other sources of range variance.

Then using Eq. 22

$$\beta_3/M = \left[1.5 \times 10^{-6} - 3.4 \times 10^{-7} \ln \frac{\langle R_1 \rangle}{M} \right] \left(\frac{\langle R_1 \rangle}{M} \right)^{2.676} \quad (23)$$

β_3 is here expressed in (microns)³. β_3 is sensitive to \bar{I} , but generally is very small.

In the expression for the mean range, two small effects enter which lead to corrections of Eq. 2. One correction arises because the more exact Eq. 20, in contrast to Eq. 1, contains the particle mass explicitly. The dependence on the mass comes about because the velocity of the fastest delta ray that can be produced depends on the mass as well as the velocity of the moving particle. The mass effect is often neglected when $\mu \gg m$, but here we must retain it, especially for mesons. The second correction is required because in the integration of Eq. 20 to obtain the range, the mean path per unit energy loss was incorrectly identified with the reciprocal of the mean rate of energy loss. The loss of energy in finite amounts in close collisions with electrons causes the range straggling, which in turn leads to the above type of error. The two corrections which together we shall call the Lewis Effect, are, therefore, both traceable to the nature of the delta ray spectrum. Allowing for them the measured mean range $\langle R_1 \rangle$ is the range R appearing in Eq. 2 increased by the factor

$$(1 + \alpha_1) \approx 1 + \frac{1}{612 M \ln 3780\beta^2}$$

If we assume $R/M = C_0 (p_1/M)^{q_0}$ to be an exact expression for the ideal quantity R , then because of the Lewis effect the value of q obtained from the proton range-energy data and the exponent q_0 differ by $\approx p_1 \frac{d\alpha_1}{dp_1}$.

For these experiments, this is only about 10^{-4} , so that correction of q for this reason is trivial. There remains, nevertheless, an uncertainty in q because of the uncertainty in the range-energy relation. The value of q , however, is not sensitive to the choice of \bar{I} . The values of q deduced from the data of Vigneron and of Bakker and Segrè are near the extremes which may be reasonably employed, so that the uncertainty in q is estimated to be of the order of one percent.

D. The Range Distribution Function

The topics treated above provide estimates of the mean range, the range variance, and range asymmetry for a particle of momentum p_1 . The form of the range distribution for essentially monoenergetic μ mesons has been studied experimentally as part of the present program. The procedure followed and the results of these measurements will be discussed in Part II.

The following statements summarize the results of the above analysis of the range and range straggling:

(a) Let R_1 be a typical measured track length, corrected by adding λ , for a particle of momentum p_1 . The mean value $\langle R_1 \rangle$ of such track lengths differs from the quantity R which satisfies Eq. 2, and the connection between the quantities is:

$$\langle R_1 \rangle = R \left(1 + \frac{a_1}{e_1} + \frac{a_2}{e_2} \right) \quad (24)$$

where $\frac{e_1}{a_1} \approx \frac{1}{612 M \ln 3780 \beta^2}$ and $\frac{e_2}{a_2} = \frac{S - S_0}{S_0} \langle \sin^2 \gamma \rangle$.

The grain-spacing correction, λ , is not made when the range is measured from a well defined point such as the terminus of a pi-meson track.

(b) The variance of R_1 will be, in good approximation:

$$\sigma_R^2 = \langle R_1^2 \rangle - \langle R_1 \rangle^2 = \beta_2^2 + \sigma_e^2 + \lambda^2 + \sigma_\gamma^2 + \sigma_d^2 \quad (25)$$

In this expression σ_e^2 is the variance introduced by personal factors in the measurement; σ_e should not exceed about $0.1 \langle R_1 \rangle^{1/2}$ for a good observer. It may be evaluated by repeated measurements on the same tracks. Here λ^2 is omitted under the same circumstances as for omission of λ above. β_2 is the important term in the present experiments.

V. STATISTICAL CALCULATION OF MASS RATIOS

Equation 6 provides the basic formula for the calculation of the mass of a particle, in units of the mass of a comparison particle. Measurements on a single meson track when compared with similar data from the track of another particle yield an estimate of their mass ratio, but because of range straggling, the finite target size, and the finite area of detector that must be employed, the measurement of particle masses can be made with much higher precision if one understands the distribution of the quantity $R_1 p^{-q}$. The empirical distribution function is found, of course, by measuring the track length, R_1 , and the apparent momentum for many particles.

If we use the average value of the observed quantity $R_1 p^{-q}$ instead of $R p^{-q}$ in Eq. 6, it leads to an apparent mass ratio M_1 , defined by:

$$M_1^{1-q} = \langle R_1 p^{-q} \rangle / \langle R_1^t p_1^{-q} \rangle$$

The connection between M_1 and the true mass ratio, M , can be obtained utilizing the information we possess regarding the various distribution functions.

As in Section III, let $U(p_1, p) dp_1$ be the probability that the momentum lies between p_1 and $p_1 + dp_1$ when the apparent momentum is p . Also let $V(R_1, p_1) dR_1$ be the probability that the observed track length will lie between R_1 and $R_1 + dR_1$ when the momentum is p_1 , and let $W(p) dp$ be the fraction of the measured values of the apparent momentum which lies between p and $p + dp$. Then the u th moment of the distribution of $R_1 p^{-q}$ may be calculated:

$$\langle R_1^u p^{-uq} \rangle = \int_p \int_{p_1} \int_{R_1} R_1^u p^{-uq} W(p) U(p_1, p) V(R_1, p_1) dp dp_1 dR_1 \quad (26)$$

For carrying out the integrations we define:

$$\langle p \rangle = \int p W(p) dp \quad \text{and} \quad \sigma_p^2 = \int (p - \langle p \rangle)^2 W(p) dp$$

Both of these quantities are obtained from the observed distribution of p . In our experiments $\sigma_p \ll \langle p \rangle$. We also note that the sign of the error in q is completely unknown so $\langle q - q_0 \rangle = 0$. We describe the uncertainty in q by an estimated standard deviation σ_q . For the same reason we take $\langle S - S_0 \rangle = 0$, and ascribe to $S - S_0$ a standard deviation σ_S .

Then from Eq. 26 we obtain several quantities of interest:

(a) The mean value of $R_1 p^{-q}$:

$$\langle R_1 p^{-q} \rangle = C_0 M^{1-q} (1 + q + \omega_q) \quad (27)$$

(b) The variance, σ^2 , of $R_1 p^{-q}$:

$$\sigma^2 = \langle R_1^2 p^{-2q} \rangle - \langle R_1 p^{-q} \rangle^2 = \langle p \rangle^{-2q} \left[\sigma_R^2 + \langle R_1 \rangle^2 (\omega_{2q} - 2\omega_q) \right] \quad (28)$$

The range straggling is dominant in the variance of $R_1 p^{-q}$.

(c) The asymmetry, Δ^3 , of $R_1 p^{-q}$:

$$\Delta^3 = \langle R_1^3 p^{-3q} \rangle - 3 \langle R_1 p^{-q} \rangle \langle R_1^2 p^{-2q} \rangle + 2 \langle R_1 p^{-q} \rangle^3$$

or

$$\Delta^3 = \langle p \rangle^{-3q} \left[\beta_3 + \langle R_1 \rangle^3 \left(\omega_{3q} - 3\omega_{2q} + 3\omega_q + 3q(2q+1) \frac{\sigma_p^2}{\langle p \rangle^2} \frac{\sigma_R^2}{\langle R_1 \rangle^2} \right) \right] \quad (29)$$

We then obtain for the mass, M :

$$M = M_1 \left[1 + \frac{\frac{e_1}{q_1} - \frac{e_1'}{q_1'}}{q - 1} + \frac{\omega_q - \omega_q'}{q - 1} \right], \quad (30)$$

We define r by setting $\langle p \rangle / \langle p' \rangle = M (1 + r)$. Then if there are n observations of $R_1 p^{-q}$ and n' observations of $R_1' p'^{-q}$, the variance, σ_M^2 , of the calculated mass is:

$$\begin{aligned}
 \sigma_M^2 = & \frac{M^2}{(q-1)^2} \left\{ \frac{\sigma^2}{n \langle R_1 p^{-q} \rangle^2} + \frac{\sigma'^2}{n' \langle R_1 p'^{-q} \rangle^2} \right. \\
 & + \frac{\sigma_q^2}{4} \left(\frac{\sigma_{p'}^2}{\langle p \rangle^2} - \frac{\sigma_{p'}^2}{\langle p' \rangle^2} - 2r \right)^2 \\
 & \left. + \frac{\sigma_S^2}{S^2} \left(\langle \sin^2 \gamma_i \rangle - \langle \sin^2 \gamma_i' \rangle \right)^2 \right\} \quad (31)
 \end{aligned}$$

Since the observed distributions of θ' and γ' are employed in calculating the mass variance, it would be incorrect to make a further statistical allowance for observational errors in these measurements.

VI. CALCULATION OF MUON DECAY MOMENTUM, ABSOLUTE MESON MASSES AND THE ELECTRIC CHARGE OF MESONS

If a pion at rest is assumed to decay only into a muon and a neutrino of zero rest mass, then the momentum, p_0 , of each disintegration product will be:

$$p_0 = \frac{a^2 - 1}{2a} \mu c, \text{ where } a \text{ is the ratio of the pion mass to the muon}$$

mass, and μ is the mass of the muon. At the same time that mass ratios are measured p_0 is also measured. One may then employ the above equation to make absolute estimates of the pion mass, the muon mass, and the pion-muon mass difference. Thus if π indicates the pion mass and μ the muon mass:

$$\mu = \frac{2a}{a^2 - 1} p_0/c \quad (32-a)$$

$$\pi = \frac{2a^2}{a^2 - 1} p_0/c \quad (32-b)$$

$$\pi - \mu = \frac{2a}{a + 1} p_0/c \quad (32-c)$$

The mass ratio a is determined in the manner described in the previous sections of this report. We can measure p_0 by comparing the ranges R_0 of muons which are observed to arise from the decay of pions stopping in the emulsion with $\langle R_1 p^{-q} \rangle$ of a comparison particle. Let the observed mean range of n_0 such muons be $\langle R_0 \rangle$. The standard deviation of the mean is then $\sigma_{R_0} / n_0^{1/2}$ where $\sigma_{R_0}^2$ is the range variance. For muons that come from the target with nearly the full decay velocity, one defines

$$K_\mu = \langle R_\mu p_\mu^{-q} \rangle \text{ and } \sigma_\mu^2 = \langle R_\mu^2 p_\mu^{-2q} \rangle - \langle R_\mu p_\mu^{-q} \rangle^2$$

If n_μ such particles are measured, then the standard deviation of K_μ amounts to

$$\sigma_\mu / n_\mu^{1/2}. \text{ We set } K_\mu \text{ equal to } K_0(1 + \omega q) \text{ where } K_0 \equiv \langle R_0 p_0^{-q} \rangle = \langle R_0 \rangle p_0^{-q}.$$

Then:

$$p_0 = \left(\frac{\langle R_0 \rangle}{K_\mu} \right)^{1/q} \left(1 + \frac{\omega q}{q} \right) \quad (33)$$

and the variance, $\sigma_{p_0}^2$, of p_0 is given by:

$$\frac{\sigma_{p_0}^2}{p_0^2} = \frac{1}{q^2} \left\{ \frac{\sigma_o^2}{\langle R_0 \rangle^2 n_o} + \frac{\sigma_\mu^2}{K_\mu^2 n_\mu} + \frac{\sigma_q^2}{4} \left(\frac{\sigma_{p_\mu}^2}{\langle p_\mu \rangle^2} + 2t \right)^2 + \frac{\sigma_S^2}{S^2} \left(\langle \sin^2 \gamma \rangle_\mu - \langle \sin^2 \gamma \rangle_o \right)^2 \right\} + \frac{\sigma_H^2}{H^2} \quad (34)$$

where $p_0/\langle p \rangle = 1 + t$, and the uncertainty in the absolute value of the magnetic field, H , is symbolized by σ_H .

Without going into minute details it may be noted that in using Eq. 32 some of the same measurements may be employed twice in obtaining α and p_0 , so that α and p_0 will not be independent. Then the expectation values and the errors in the calculated masses must be obtained by rewriting the expressions so that the mass formulas contain only independent measurable quantities. On the other hand, p_0 also may be determined by comparing K_0 with

$K_\pi = \langle R_\pi p_\pi^{-q} \rangle$, obtained from measurements of pion tracks in the same plate in which the tracks of decay muons are measured. In this case α , obtained from an independent experiment, is employed so that α , K_π , and $\langle R_0 \rangle$ are all independent. For the measurement of p_0 , the absolute value of the magnetic field intensity is required, and the uncertainty in the field measurement must be compounded with the statistical error. Finally, if the velocity of the decay muon is not the same as the mean velocity of the comparison particle, the uncertainty in q again enters the calculated error.

The mass ratio method and the absolute calculations based on the measurement of p_0 provide two independent estimates of the positive pion mass. These depend on the meson electric charge in different ways, so a limit may be put on the deviation of the meson charge from that of the proton. For simplicity, we assume that the charge of the positive pion and muon each differ by the factor

$(1 + \epsilon)$ from the charge of the proton. Then the ratio of the derived absolute π^+ mass to the mass obtained from the mass ratio method will be $\approx 1 - \frac{\epsilon}{q-1}$. The results quoted in Parts II and III agree very well, but the ratio is uncertain by about 0.4 percent. From these experiments alone, therefore, we can deduce only that the meson charge is equal to the proton charge to within about one percent.

VII. RESIDUAL EFFECTS

Equations 30 and 31 enable one to calculate the mass and its statistical reliability. There remains, however, the possibility of unknown sources of error. Equations 28 and 29 provide measures of the distribution of R_p^{-q} which can be compared with those actually found. If they are significantly different it may be possible to trace the difference to an overlooked effect which could influence the results. In this way, contamination of the mesons with particles which did not come from the target has been detected in the distribution of R_p^{-q} observed in an earlier experiment.^{4c} The background mesons had the effect of raising the apparent mass by an amount that exceeded the statistical probable error of those measurements. In the present experiments, steps have been taken to eliminate this background, and it is certain that the contamination has been greatly reduced.

We have assumed that the stopping cross section for a charged particle in matter is independent^{3a} of the sign of the particle, and that the absolute magnitude of the electric charge of the various kinds of mesons is the same as that of the proton. It has also been assumed that the stopping can be calculated in sufficient approximation allowing solely for electromagnetic effects. Should these assumptions be inexact, this inexactness may be revealed by discrepancies between the present results and precise measurements made by other means.

The errors in measuring linear dimensions of the apparatus and the shape of the magnetic field distribution have not been included in Eq. 31. The experiments were designed so that these effects should not be large enough to affect the results.

ACKNOWLEDGEMENTS

The original stimulation for this endeavor was the work of E. Gardner and C. M. G. Lattes, and their ideas have been retained in some of the experimental procedures. Before poor health forced the discontinuance of his work, many aspects of the new measurements were planned in extended discussions with Dr. E. Gardner. In working out the details of the theoretical arguments, I have leaned heavily on the sound criticisms of my associates, F. M. Smith and W. Birnbaum, who carried the main load in the measurement program. Throughout the extended period required to complete this work, Professor E. O. Lawrence continued his sympathetic support.

REFERENCES

1. Many of the earlier measurements are reviewed in the following:
 - (a) J. A. Wheeler and R. Ladenburg, *Phys. Rev.* 60, 754 (1941).
 - (b) C. F. Powell, *Rep. Prog. Phys.* 13, 350 (1950)
(London: Physical Society).
2. P. E. Hodgson, *Phil. Mag.* 41, 725 (1950) and J. K. Bowker, J. R. Green, and W. H. Barkas, *Phys. Rev.* 81, 649 (1951).
3. Some of the meson mass measurements by grain count and range were made by the following: C. M. G. Lattes, G. P. S. Occhialini, and C. F. Powell, *Proc. Phys. Soc. London* 61, 173 (1948); L. Van Rossum, *Comptes Rendus* 228, 676 (1949); and J. K. Bowker, *Phys. Rev.* 78, 87 (1950).
4. The present mass ratio method has been partially described and progress reported in the following:
 - (a) W. H. Barkas, UCRL Memorandum, 12 May, 1949.
 - (b) W. H. Barkas, Proceedings of the Echo Lake Cosmic Ray Symposium, June 23, 1949.
 - (c) W. H. Barkas, F. M. Smith, and E. Gardner, *Phys. Rev.* 82, 102 (1951).
 - (d) W. Birnbaum, F. M. Smith, and W. H. Barkas, *Phys. Rev.* 83, 895(A) (1951).
 - (e) W. H. Barkas, *Amer. Jour. of Phys.* 20, 5 (1952).
 - (f) F. M. Smith, W. Birnbaum and W. H. Barkas, *Phys. Rev.* 91, 765 (1953).
5. R. B. Brode, *Rev. Mod. Phys.* 21, 37 (1949), *Phys. Rev.* 75, 904 (1949); W. B. Fretter, *Phys. Rev.* 70, 625 (1946); J. G. Retallack and R. B. Brode, *Phys. Rev.* 75, 1716 (1949); T. C. Merkle, E. L. Goldwasser, and R. B. Brode, *Phys. Rev.* 79, 926 (1950); G. M. Nonnemaker and J. C. Street, *Phys. Rev.* 82, 564 (1951); C. Franzinetti, *Phil. Mag.* 41, 86 (1950); I. Barbour, *Phys. Rev.* 78, 518 (1950); G. Ascoli, *Phys. Rev.* 90, 1079 (1953).
6. Examples: E. J. Williams and E. Pickup, *Nature* 141, 648 (1938); D. R. Corson and R. B. Brode, *Phys. Rev.* 53, 215, 773 (1938); and J. C. Street and E. C. Stevenson, *Phys. Rev.* 52, 1003 (1937).
7. S. Lattimore, *Nature* 161, 518 (1948) and Y. Goldschmidt-Clermont, D. T. King, H. Muirhead, and D. M. Ritson, *Proc. Phys. Soc.* 61, 183 (1948).

X 7. R. B. Leighton, C. D. Anderson, and A. J. Seriff, Phys. Rev. 75, 1432 (1949); A. Lagarrigue and C. Peyron, Comptes Rendus 233, 478 (1951); J. H. Davies, W. O. Lock and H. Muirhead, Phil. Mag. 40, 1250 (1949); H. J. Bramson, A. M. Seifert, W. W. Havens, Jr., Phys. Rev. 88, 304 (1952); and R. Sagane, W. L. Gardner, and H. W. Hubbard, Phys. Rev. 82, 557 (1951). +

8. V. Z. Peterson, E. Iloff, and D. Sherman, Phys. Rev. 81, 647 (1951), and W. F. Cartwright, Phys. Rev. 82, 460 (1951).

X 9. W. K. H. Panofsky, R. L. Aamodt, and J. Hadley, Phys. Rev. 81, 565 (1951), and K. M. Crowe, Thesis, University of California (1952).

X 10. J. Rainwater, Phys. Rev. 90, 349 (1953).

X 11. M. S. Livingston and H. H. Bethe, Rev. Mod. Phys. 9, 263 (1937).

12. J. Thibaud, Phys. Rev. 45, 781 (1934).

13. W. H. Barkas, Phys. Rev. 78, 90 (1950).
14. w. H. Barkas UCRL 2327

15. W. Heitler, Quantum Theory of Radiation, Oxford, 1944, p. 172.

~~16. E. Fermi, Nuclear Physics, p. 36, University of Chicago Press, Chicago 1950.~~
16. Barkas et al. Phys Rev April 1 1955

~~17. M. J. Berger, Phys. Rev. 88, 59 (1952).~~

~~18. H. Bradner, F. M. Smith, W. H. Barkas, and A. S. Bishop, Phys. Rev. 77, 462 (1950).~~

~~19. C. J. Bakker and E. Segre, Phys. Rev. 81, 489 (1951).~~

~~20. P. Cüer, C. R. Acad. Sc. 223, 1121 (1946).~~

21. J. J. Wilkins, Atomic Energy Research Establishment (Harwell) Report G/R 664 (1951) (unpublished)

~~22. J. Rotblat, Nature 167, 550 (1951).~~

23. A. Oliver, UCRL Report 2176, April 6, 1953.

18 24. L. Vigneron, Journ. de Physique 14, 145 (1953).

19 ~~24~~ 25. W. H. Barkas, Phys. Rev. 89, 1019 (1953).

26. N. Bohr, Phil. Mag. 30, 581 (1915).

27. H. Cramer, Mathematical Methods of Statistics, Princeton University Press, Princeton, 1946.

20 ~~28~~ 28. H. W. Lewis, Phys. Rev. 85, 20 (1952).

29. L. Winand, Photographic Sensitivity, p. 288, Butterworths, London, 1951.

30. A. M. Seifert, Private Communication.

31. W. F. Fry and G. R. White, Phys. Rev. 90, 207 (1953).

21 Equibi etc.

22 Fry

32. Because matter is unsymmetrical with respect to electric charge, it is reasonable to suppose that in some order of approximation the stopping cross section will depend on the sign of the moving particle. Professor E. Fermi has pointed out that the Mott theory of electron scattering provides an unambiguous prediction of such an effect. He has kindly calculated the magnitude of the effect to be anticipated in our experiments. It should appear as an apparent reduction of the negative pion mass with respect to that of the positive pion by about one part in a thousand.